RSC Advances

This is an *Accepted Manuscript*, which has been through the Royal Society of Chemistry peer review process and has been accepted for publication.

Accepted Manuscripts are published online shortly after acceptance, before technical editing, formatting and proof reading. Using this free service, authors can make their results available to the community, in citable form, before we publish the edited article. This *Accepted Manuscript* will be replaced by the edited, formatted and paginated article as soon as this is available.

You can find more information about *Accepted Manuscripts* in the Information for Authors.

Please note that technical editing may introduce minor changes to the text and/or graphics, which may alter content. The journal's standard Terms & Conditions and the Ethical guidelines still apply. In no event shall the Royal Society of Chemistry be held responsible for any errors or omissions in this *Accepted Manuscript* or any consequences arising from the use of any information it contains.

ROYAL SOCIETY OF CHEMISTRY

www.rsc.org/advances

CREATED USING THE RSC ARTICLE TEMPLATE (VER. 3.1) - SEE WWW.RSC.ORG/ELECTRONICFILES FOR DETAILS

ARTICLE TYPE www.rsc.org/xxxxxx | XXXXXXXX

Polymeric templates and solvent effects: syntheses and properties of polymeric iodoargentates containing solvated $[Mn(4,4'\text{-bpy})]^{2+}$ cations

Yali Shen, Jialin Lu, Chunying Tang, Wang Fang, Yong Zhang and Dingxian Jia*

Received (in XXX, XXX) Xth XXXXXXXXX 200X, Accepted Xth XXXXXXXXX 200X
First published on the web Xth XXXXXXXXX 200X
DOI: 10.1039/b000000x

Four new polymeric iodoargentates were prepared by the reactions of AgI and KI templated by solvated $[Mn(4,4'\text{-bpy})]^{2+}$ complex cation in different mixed solvents. The reaction in DMF/H_2O, DMSO/H_2O, and DMF/DMSO/H_2O (DMF = dimethylformamide; DMSO = dimethylsulfoxide) produced $[Mn(4,4'\text{-bpy})(DMF)_3(H_2O)]Ag_5I_7\cdot 4,4'\text{-bpy}$ (**1**), $[Mn(4,4'\text{-bpy})(DMSO)_4]_2Ag_{11}I_{15}$ (**2**), $[Mn(4,4'\text{-bpy})_2(DMSO)_2(H_2O)_2]Ag_{10}I_{12}\cdot 2DMSO\cdot 2H_2O$ (**3**), and $[Mn_2(4,4'\text{-bpy})_2(DMF)_5(DMSO)_2(H_2O)]Ag_{10}I_{14}\cdot 2DMF$ (**4**) (4,4′-bpy = bipyridine), respectively. In **1**, four AgI_4 units are joined by sharing common edges forming a Ag_4I_9 fragment. The Ag_4I_9 fragments are connected into a 1-D $[Ag_5I_7^{2-}]_n$ polymeric anion by a AgI_4 unit. In **2**, six AgI_4 units share common edges to form $[Ag_6I_{12}]_n$ chain-like subunits. Two $[Ag_6I_{12}]_n$ subunits are joined by μ-I bridges, forming a novel ladder-shaped $[Ag_{11}I_{15}^{4-}]_n$ polymeric anion. The $[Ag_{10}I_{12}^{2-}]_n$ in **3** is composed of a circular Ag_5I_{12} subunit via sharing five terminal iodine atoms. Two Ag_4I_9 and one Ag_2I_4 fragments are interjoined via sharing common face to form the 1-D $[Ag_{10}I_{14}^{4-}]_n$ anion in **4**. Compounds **1**, **2** and **4** are the first examples of iodoargentates containing polymeric counter cations. The stronger Ag···Ag interactions in the $[Ag_{11}I_{15}^{4-}]_n$ and $[Ag_{10}I_{14}^{4-}]_n$ anions cause red-shift in the luminescent spectra of compounds **2** and **4**, compared with those of **1** and **3**.

Introduction

Interest in organic−inorganic hybrid halometallates of heavy metals originates not only from their wide range of intriguing structural topologies but also from the opportunity to combine useful properties of both components, and the possibility to tune the physical properties by the organic components to form functional materials.[1,2] The chemistry of silver(I) iodide organic–inorganic hybrid complexes have received special attention for their tunable structural owing to the strong affinity of Ag(I) for the iodine anion and interesting physical properties. The high tendency for self-assembly of the AgI_4 units via corner-, edge-, or face-sharing lead to different compositions and structures ranging from isolated anions to extended arrays dependent on the templates or counter cations used in the synthesis. Much effort in exploratory templating synthesis has led to a large number of iodoargentate anions with different dimensional structures using a variety of organic cations as structure directing agents.[3] Transition metal complex cationic templates $[Cu(en)_2]^{2+}$ and $[TM(en)_3]^{2+}$ (TM = Ni, Zn; en = ethylenediamine) have led to compounds $[Cu(en)_2][Ag_2I_4]$ and $[TM(en)_3][Ag_2I_4]$ in dimethylformamide, which contain one-dimensional (1-D) $[Ag_2I_4^{2-}]_n$ chain and three-dimensional (3-D) $[Ag_2I_4^{2-}]_n$ network, respectively.[4, 5] Recently, a 1-D $[Ag_{10}I_{12}^{2-}]_n$ anion has been obtained in the presence of $[Ni(2,2'\text{-bpy})(THF)_2(H_2O)_2]^{2+}$ complex cation.[6] A third class of iodoargentates is based on lanthanide (Ln) complex counter ions, an area dominated by the work of Mishra and co-workers.[7] A number of iodoargentates containing solvated Ln(III) cations were isolated from DMF or DMSO solvents. In the syntheses of the metal-containing iodoargentates, the TM or Ln complexes formed *in situ* act as space fillers and/or charge compensating ions in the final iodoargentates. Compared with the extensively investigated iodoargentates with organic cations, the iodoargentate with metal-organic cations remains less explored. Furthermore, all above iodoargentates were prepared templated by discrete cations. As far as we know, the synthesis of iodoargentates using polymeric cations as templates has not been reported before.

It has been documented that the compositions, structures and dimensionalities of halometallates are sensitive to specific reaction conditions, such as reaction temperature, reactant concentrations, solvents and crystallization conditions, and to the nature and size of the templates or counterions used for crystallization.[8] The high tendency for self-assembly of the AgI_4 tetrahedron provides a wide selection of reaction conditions and counterions in design and preparation of new iodoargentates. In this manuscript, we chose the $[Mn(4,4'\text{-bpy})]^{2+}$ complex cation modified by small ligands via solvating in different polar solvents, to fine-tune the assembling of AgI_4 unit. The reaction of AgI, KI, $MnCl_2\cdot 4H_2O$ and 4,4′-bipyridine (4,4′-bpy) in different mixed solvents afforded a series of polymeric iodoargentates $[Mn(4,4'\text{-bpy})(DMF)_3(H_2O)]Ag_5I_7\cdot 4,4'\text{-bpy}$ (**1**), $[Mn(4,4'\text{-bpy})(DMSO)_4]_2Ag_{11}I_{15}$ (**2**), $[Mn(4,4'\text{-bpy})_2(DMSO)_2(H_2O)_2]Ag_{10}I_{12}\cdot 2DMSO\cdot 2H_2O$ (**3**), and $[Mn_2(4,4'\text{-bpy})_2(DMF)_5(DMSO)_2(H_2O)]Ag_{10}I_{14}\cdot 2DMF$ (**4**). In the syntheses, all Mn^{2+} ions are coordinated by 4,4′-bpy and solvated by solvent moleclues to form mixed-coordinated polymeric cations in **1**, **2** and **4**, or mononuclear complex cation in **3**. Compounds **1**, **2** and **4** are the first examples of iodoargentates containing polymeric cations. Herein, we

RSC Advances Accepted Manuscript

report the syntheses, crystal structures, and solid-state optical absorption, luminescent and thermal properties of compounds **1**–**4**.

Experimental

Materials and General Methods

All starting materials were of analytical grade and were used as received. Elemental analyses were performed using an EA1110-CHNS-O elemental analyzer. Fourier-transform infrared (FT-IR) spectra were recorded with a Nicolet Magna-IR 550 spectrometer, using dry KBr discs, in the range of 4000–400 cm^{-1}. Powder X-ray diffraction (PXRD) patterns were collected on a D/MAX-3C diffractometer using graphite monochromatized CuKα radiation (λ = 1.5406 Å). Room-temperature optical diffuse reflectance spectra of the powdered samples were obtained using a Shimadzu UV-3150 spectrometer. The absorption (α/S) data were calculated from the reflectance using the Kubelka-Munk function $\alpha/S = (1 - R)^2/2R$,[9] where R is the reflectance at a given energy, α is the absorption, and S is the scattering coefficient. Photoluminescence spectra of the crystalline samples were recorded on a F-2500 FL spectrophotometer with wavelength increment 1.0 nm at room temperature using a xenon arc lamp as the excitation source. Thermal gravimetric analyses (TGA) were conducted on an SDT 2960 microanalyzer; the samples were heated at a rate of 5 ºC min^{-1} under a nitrogen stream of 100 mL min^{-1}.

Syntheses of 1–4

$[Mn(4,4'\text{-bpy})(DMF)_3(H_2O)]Ag_5I_7\cdot 4,4'\text{-bpy}$ (1). $MnCl_2\cdot 4H_2O$ (0.099 g, 0.5 mmol), and 4,4′-bpy·$2H_2O$ (0.096 g, 0.5 mmol) were dissolved in 3 mL of DMF/H_2O (volume ration 2:1) mixed solvent by stirring and a yellowish solution was obtained. 5 mL of DMF solution containing AgI (0.235 g, 1.0 mmol) and KI (0.249 g, 1.5 mmol) was added drop wise to the above solution. After stirring for 2 h, the mixture was filtered. The filtrate was kept at room temperature for about one week, and prismatic crystals of **1** were obtained. The crystals were filtered off, washed with ethanol and stored under a vacuum (75% yield based on AgI). Elem. Anal. Calcd for $C_{29}H_{39}N_7O_4MnI_7Ag_5$ (**1**): C, 17.14; H, 1.93; N, 4.82; found: C, 17.01; H, 1.84; N, 4.68%. IR data (KBr, cm^{-1}): 3068(w), 2286(w), 1660(s), 1598(s), 1569(w), 1470(m), 1436(s), 1384(w), 1308(m), 1247(w), 1160(m), 1096(w), 1017(m), 903(w), 764(s), 733(m), 651(w), 578(w), 511(w), 410 (w).

$[Mn(4,4'\text{-bpy})(DMSO)_4]_2Ag_{11}I_{15}$ (2). $MnCl_2\cdot 4H_2O$ (0.099 g, 0.5 mmol), and 4,4′-bpy·$2H_2O$ (0.096 g, 0.5 mmol) were dissolved in 3 mL of DMSO/H_2O (volume ration 2:1) by stirring and a light yellow solution was obtained. 3 mL of DMSO solution containing AgI (0.235 g, 1.0 mmol) and KI (0.249 g, 1.5 mmol) was added drop wise to the above solution. After stirring for 2 h, the mixture was filtered. The filtrate was kept at room temperature for about one week, and block crystals of **2** were obtained. The crystals were filtered off, washed with ethanol and stored under a vacuum (57% yield based on AgI). Elem. Anal. Calcd for $C_{36}H_{64}O_8S_8Mn_2I_{15}Ag_{11}$ (**2**): C, 10.45; H, 1.56; N, 1.35; found: C, 10.38; H, 1.48; N, 1.21%. IR data (KBr, cm^{-1}): 3072(w), 2346(w), 1980(w), 1594(m), 1466(w), 1436(s), 1304(m), 1251(w), 1157(m), 1104(w), 1010(s), 899(w), 817(w), 764(s), 733(s), 651(m), 521(w), 439(w), 412(w).

$[Mn(4,4'\text{-bpy})_2(DMSO)_2(H_2O)_2]Ag_{10}I_{12}\cdot 2DMSO\cdot 2H_2O$ (3). $MnCl_2\cdot 4H_2O$ (0.099 g, 0.5 mmol), and 4,4′-bpy·$2H_2O$ (0.096 g, 0.5 mmol) were dissolved in 3 mL of DMSO/H_2O (volume ration 1:1) mixed solvent by stirring and a yellowish solution was obtained. 3 mL of DMSO solution containing AgI (0.235 g, 1.0 mmol) and KI (0.249 g, 1.5 mmol) was added drop wise to the above solution. After stirring for 2 h, the mixture was filtered. The filtrate was kept at room temperature for about one week, and prismatic crystals of **3** were obtained. The crystals were filtered off, washed with ethanol and stored under a vacuum (64% yield based on AgI). Elem. Anal. Calcd for $C_{29}H_{39}N_7O_4MnI_{12}Ag_{10}$ (**3**): C, 10.03; H, 1.44; N, 1.67; found: C, 9.89; H, 1.32; N, 1.58%. IR data (KBr, cm^{-1}): 3068(w), 2362(w), 2335(w), 1663(w), 1602(m), 1564(w), 1466(m), 1440(s), 1311(m), 1270(w), 1239(m), 1157(m), 1119(w), 1036(w), 884(w), 802(w), 760(s), 729(m), 651(w), 563(w), 420(w).

$[Mn_2(4,4'\text{-bpy})_2(DMSO)_2(DMF)_5(H_2O)]Ag_{10}I_{14}\cdot 2DMF$ (4). $MnCl_2\cdot 4H_2O$ (0.099 g, 0.5 mmol), and 4,4′-bpy·$2H_2O$ (0.096 g, 0.5 mmol) were dissolved in 3 mL of DMSO/DMF/H_2O (volume ration 1:1:1) mixed solvent by stirring and a yellowish solution was obtained. 4 mL of DMSO/DMF (volume ration 1:1) solution containing AgI (0.235 g, 1.0 mmol) and KI (0.249 g, 1.5 mmol) was added drop wise to the above solution. After stirring for 2 h, the mixture was filtered. The filtrate was kept at room temperature for about one week, and block crystals of **4** were obtained. The crystals were filtered off, washed with ethanol and stored under a vacuum (68% yield based on AgI). Elem. Anal. Calcd for $C_{45}H_{79}N_{11}O_{10}S_2Mn_2I_{14}Ag_{10}$ (**4**): C, 13.64; H, 2.01; N, 3.89; found: C, 13.48; H, 1.95; N, 3.81%. IR data (KBr, cm^{-1}): 3060(w), 2925(w), 2849(w), 1745(w), 1663(s), 1594(m), 1519(w), 1466(m), 1436(s), 1304(w), 1247(w), 1157(w), 1096(w), 1054(w), 1013(m), 964(w), 874(w), 771(s), 737(m), 691(w), 647(w), 597(w), 552(w), 507(w), 458(w), 412(m).

X-ray Crystal Structure Determinations

All data were collected on a Rigaku Saturn (**1**, **3**, **4**) or a Rigaku Mercury (**2**) CCD diffractometer using graphite-monochromated Mo-$K\alpha$ radiation (λ = 0.71073 Å) in ω-scanning mode, to a maximum 2θ of 50.70º. An empirical absorption correction was applied to the data. The structures were solved using SHELXS-97,[10a] and refinement was performed against F^2 using SHELXL-97.[10b] All the non-hydrogen atoms were refined anisotropically. The hydrogen atoms were added geometrically and refined using a riding model. The S(3) and S(4) atoms in **2** are disordered. The occupancies of the disordered atoms are refined as 73% and 27% for S(3), and 54% and 46% for S(4). The occupancies of the disordered atoms C(20), C(31)–C(33) and C(38)–C(39) in **4** are refined as 55% and 45%, 58% and 42% , and 52% and 48%, respectively. Crystallographic, experimental, and

RSC Advances Accepted Manuscript

This journal is © The Royal Society of Chemistry [year]

analytical data for the title compounds are listed in Table 1.

Table 1 Crystallographic and refinement of **1**–**4**

	1	**2**	**3**	**4**
Empirical Formula	$C_{29}H_{39}N_7O_4MnAg_5I_7$	$C_{36}H_{64}N_4O_8S_8Mn_2Ag_{11}I_{15}$	$C_{28}H_{48}N_4O_8S_4MnAg_{10}I_{12}$	$C_{45}H_{79}N_{11}O_{10}S_2Mn_2Ag_{10}I_{14}$
Formula weight	2032.26	4137.34	3353.38	3963.49
Crystal system	Monoclinic	Monoclinic	Monoclinic	Triclinic
Space group	$P\,2_1$ (no. 4)	$P\,2_1/n$ (no. 14)	$P\,2_1/c$ (no. 14)	P –1
a/ Å	11.7091(18)	8.2323(12)	16.3520(11)	13.0276(18)
b/ Å	15.066(2)	34.488(5)	7.8920(5)	16.091(2)
c/ Å	13.811(2)	15.856(2)	27.221(2)	22.994(5)
β/ º	96.441(4)	94.218(4)	100.299(2)	86.076(14)
V/ Å^3	2421.1(7)	4489.6(11)	3456.3(4)	4608.8(13)
Z	2	2	2	2
T/ K	223(2) K	293(2)	223(2)	223(2) K
Measured reflections	12364	36858	27056	36645
Independent reflections	8000	8164	6323	16758
R_{int}	0.0318	0.0740	0.0476	0.0601
Parameters	456	402	309	699
$R1$ [$I > 2\sigma(I)$]	0.036	0.0411	0.0474	0.0584
*wR*2 (all data)	0.0700	0.1350	0.0869	0.1418
Goodness of fit	0.977	1.013	1.193	1.127

Results and Discussion

Syntheses and IR Spectra.

Title compounds were prepared by the reaction of AgI, KI, $MnCl_2{\cdot}4H_2O$ and 4,4′-bpy in different mixed polar solvents at ambient temperature (Scheme 1). Reactions of AgI, KI, $MnCl_2{\cdot}4H_2O$ and 4,4′-bpy in mixed solvents DMF/H_2O and DMSO/H_2O (volume ration 2:1) produced compounds $[Mn(4,4'\text{-bpy})(DMF)_3(H_2O)]Ag_5I_7{\cdot}4,4'\text{-bpy}$ (**1**) and $[Mn(4,4'\text{-bpy})(DMSO)_4]_2Ag_{11}I_{15}$ (**2**), respectively. The increase of H_2O in preparation of **2** gave a new compound $[Mn(4,4'\text{-bpy})_2(DMSO)_2(H_2O)_2]Ag_{10}I_{12}{\cdot}2DMSO{\cdot}2H_2O$ (**3**), in which H_2O solvent molecules besides DMSO are integrated in the Mn^{2+} complex as the H_2O molecules occur in **1**. The reaction in triple DMF/DMSO/H_2O mixed solvent produced compound $[Mn_2(4,4'\text{-bpy})_2(DMF)_5(DMSO)_2(H_2O)]Ag_{10}I_{14}{\cdot}2DMF$ (**4**), simultaneously containing DMF, DMSO and H_2O three coordinated solvent ligands. Summarily, the $[Mn(4,4'\text{-bpy})]^{2+}$ units are solvated by DMF, DMSO and/or H_2O solvent molecules to form mixed coordinated complexes in **1**–**4**. The purity of bulk phases of compounds **1**–**4** are investigated using powder X-ray diffraction (PXRD). The PXRD patterns of the bulk phases of **1**–**4** are consistent with the simulated PXRD patterns based on single-crystal XRD data (Fig.s S1–S4 †), respectively.

The FT-IR spectra show characteristic absorptions from the DMF, DMSO, and 4,4′-bpy ligands on the Mn^{2+} ions (Fig.s S5–S8 †). Compounds **1** and **4** show an intense C=O vibration in the frequency range 1655–1663 cm^{-1}. The C–N stretching vibrations are at about 1096 cm^{-1}. The intense absorptions in the frequency range 1010–1013 cm^{-1} in compounds **2**, **3** and **4** are attributed to the S=O vibrations. The vibrations of pyridine ring in compounds **1**–**4** occur between 1579 cm^{-1} and 1598 cm^{-1}.

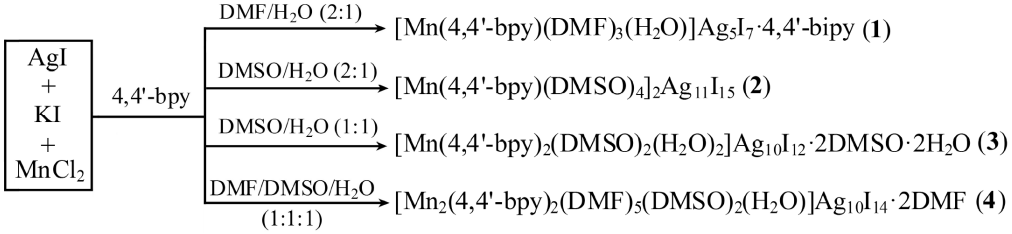

Scheme 1. Syntheses of compounds **1**–**4**.

Crystal Structures of 1−4.

Compound **1** crystallizes in the monoclinic space group $P2_1$ with two formula units in the unit cell. It consists of a 1-D polymeric iodoargentate anion $[Ag_5I_7^{2-}]_n$, and 1-D polymeric $[Mn(4,4'\text{-bpy})(DMF)_3(H_2O)]^{2+}$ counter cation, as well as a free 4,4′-bpy molecule. The Mn^{2+} ion binds three DMF and one H_2O molecules, forming a $[Mn(DMF)_3(H_2O)]^{2+}$ fragment. The $[Mn(DMF)_3(H_2O)]^{2+}$ fragments are bridged by a 4,4′-bpy ligand, generating the linear coordination polymer $\{[Mn(4,4'\text{-bpy})(DMF)_3(H_2O)]^{2+}\}_n$ (Fig. 1). The Mn^{2+} ion is in a slightly distorted octahedral geometry with axial angles in the range of 175.1(3)–177.7(3)° (Table S1†). The Mn–N bond lengths are 2.303(7) and 2.314(7) Å, while the Mn–O bond lengths are in

RSC Advances Accepted Manuscript

2.138(7)–2.184(8) Å (Tables S1). The Mn–N and Mn–O bond lengths are in accordance with those of Mn-complexes containing bpy and DMF ligands, respectively.[11]

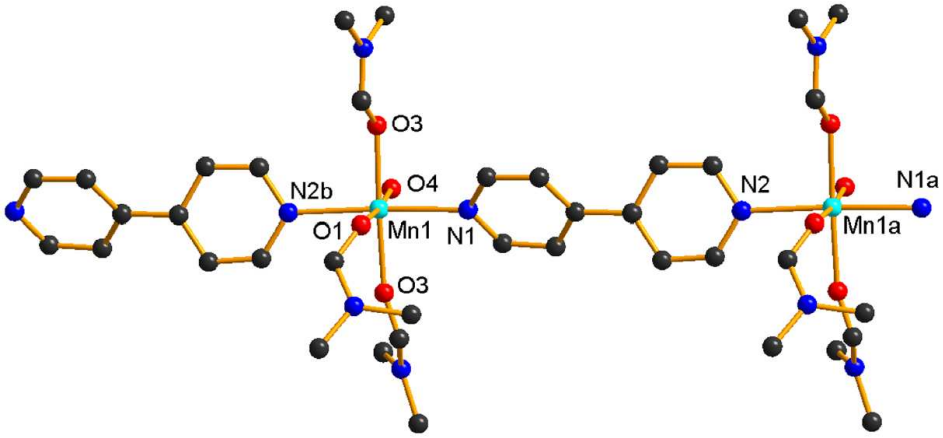

Fig. 1 Crystal structure of the coordination polymer $\{[Mn(4,4'\text{-bpy})(DMF)_3(H_2O)]^{2+}\}_n$ in **1** with labeling scheme. Hydrogen atoms are omitted for clarity.

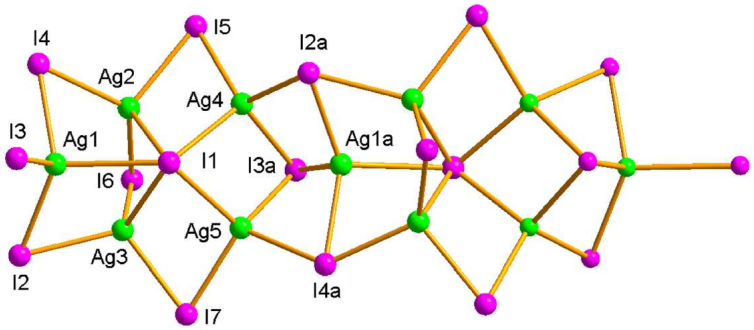

Fig. 2 Crystal structure of the $[Ag_5I_7^{2-}]_n$ chain in **1** with the labeling scheme.

The $[Ag_5I_7^{2-}]_n$ polymeric anion contains five crystallographically independent Ag^+ ions, and seven iodine anions (Fig. 2). All Ag(I) ions are coordinated to four iodine anions at distances in the range of 2.7461(11)–3.1878(12) Å, forming distorted tetrahedral AgI_4 units with I–Ag–I angles in the range of 95.43(3)–127.25(3)° (Table S1†). The bond lengths and bond angles of the AgI_4 tetrahedra are in agreement with those of reported iodoargentates.[3–7] As shown in Fig. 2, four AgI_4 (containing Ag2, Ag3, Ag4, Ag5) units are connected by sharing common edges to form a circular Ag_4I_9 fragment, in which I1 shares five Ag^+ ions. The Ag_4I_9 fragments are joined by the fifth Ag(1)I_4 unit via sharing I1, I2, I3, and I4 atoms, to form the 1-D $[Ag_5I_7^{2-}]_n$ polymeric anion. There are no terminal iodide anions in the $[Ag_5I_7^{2-}]_n$ anion. The iodide anions adopt μ_5-I (I1), μ_3-I (I2, I3, I4) and μ-I (I5, I6, I7) bridging coordination modes to the Ag(I) ions. Correspondingly, the Ag–I bond lengths decrease in the order Ag–μ_5-I [av.: 3.0177(10) Å] > Ag–μ_3-I [av.: 2.8737(10) Å] > Ag–μ-I [av.: 2.7738(11) Å]. Short Ag···Ag distances of 3.1181(14) and 3.1986(14) Å, which are shorter than the sum of the van der Waals radii of 3.44 Å,[12] are observed in the $[Ag_5I_7^{2-}]_n$ chain (Table S1†), indicating metal-metal interactions.

In **1**, the free 4,4′-bpy molecules run along the $\{[Mn(4,4'\text{-bpy})(DMF)_3(H_2O)]^{2+}\}_n$ chain. The pyridine planes of the coordinated and free 4,4′-bpy molecules are parallel to each other, with interplane distance of 3.361 Å, indicating weak π–π stacking interaction (Fig. S9†). The free 4,4′-bpy molecules are connected end to end by the H_2O molecules of $\{[Mn(4,4'\text{-bpy})(DMF)_3(H_2O)]^{2+}\}_n$ via N–H···O [N···O: 2.742(10), 2.777(12) Å] (Table S5†) interactions. As a result, a cationic chain $\{[Mn(4,4'\text{-bpy})(DMF)_3(H_2O)]^{2+}\cdot 4,4'\text{-bpy}\}_n$ is formed (Fig. S9†). The cationic $\{[Mn(4,4'\text{-bpy})(DMF)_3(H_2O)]^{2+}\cdot 4,4'\text{-bpy}\}_n$ and anionic $[Ag_5I_7^{2-}]_n$ chains run perpendicular to each other, forming a penetrating crystal lattice work (Fig. 3, Fig. S10†).

RSC Advances Accepted Manuscript

This journal is © The Royal Society of Chemistry [year]

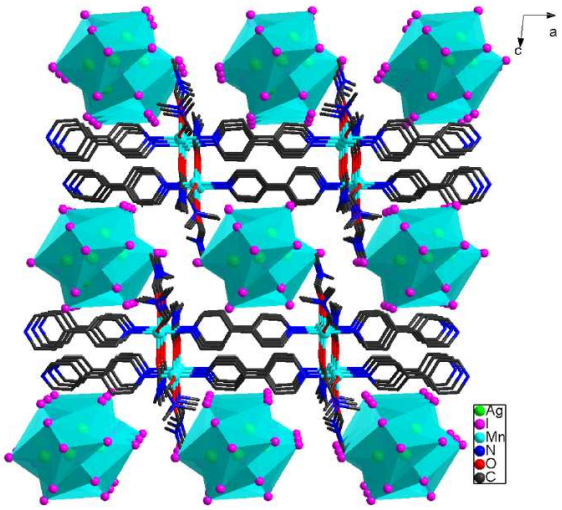

Fig. 3 View of **1** along the *b* axis. The AgI_4 units are shown as blue tetrahedra. Hydrogen atoms are omitted for clarity.

Compound **2** crystallizes in the monoclinic space group $P2_1/n$ (Table 1). It is composed of polymeric $\{[Mn(4,4'\text{-bpy})(DMSO)_4]^{2+}\}_n$ cation, and $[Ag_{11}I_{15}^{4-}]_n$ anion. Four DMSO molecules coordinate to the Mn^{2+} ion via O-donor atom, forming a $[Mn(DMSO)_4]^{2+}$ unit. The $[Mn(DMSO)_4]^{2+}$ units are joined by 4,4′-bpy ligands, generating a novel zigzag coordination polymer $\{[Mn(4,4'\text{-bpy})(DMSO)_4]^{2+}\}_n$ (Fig. 4). The Mn^{2+} ion forms a slightly distorted octahedron MnN_2O_4 with axial angle in the range of 171.1(5)–79.2(6)° (Table S2†). Unlike the 4,4′-bpy ligand in **1** which connects the $[Mn(DMF)_3(H_2O)]^{2+}$ fragments into a linear coordination polymer $\{[Mn(4,4'\text{-bpy})(DMF)_3(H_2O)]^{2+}\}_n$ (Fig. 1), the 4,4′-bpy ligand leads to a zigzag coordination polymer $\{[Mn(4,4'\text{-bpy})(DMSO)_4]^{2+}\}_n$ (Fig. 4) in which two N atoms are at the *cis* position of the MnN_2O_4 octahedron. The Mn–N and Mn–O bond lengths are similar to the corresponding bond lengths in **1** (Table S1 and S2†). Compound **2** contains five and a half crystallographically independent Ag^+ ions, and seven and a half iodine anions (Fig. 5). All Ag^+ ions are tetrahedrally coordinated to four iodine anions at distances in the range of 2.800(3)–3.052(3) Å. Five AgI_4 (containing Ag1, Ag2, Ag3, Ag4, Ag5) units are connected by sharing common edges to form an Ag_5I_{10} fragment, in which I1 shares four Ag^+ ions. The Ag_5I_{10} fragments are joined by the $Ag(6)I_4$ units via sharing I3, I4, I6 (concerning Ag2, Ag3, Ag5), and I3, I6, I7 (concerning Ag1, Ag4, Ag5) atoms, to form the 1-D $[Ag_6I_{12}]_n$ chain. Two $[Ag_6I_{12}]_n$ chains are joined by sharing μ-I8, forming a novel ladder-shaped $[Ag_{11}I_{15}^{4-}]_n$ polymeric anion (Fig. 5). The $[Ag_{11}I_{15}^{4-}]_n$ polymeric anion contains 12-membered Ag_6I_6 rings. Iodine anions adopt μ-I (I2, I8), μ_3-I (I3, I5, I6) or μ_4-I (I1, I4, I7) bridging coordination modes in the $[Ag_{11}I_{15}^{4-}]_n$ chain.

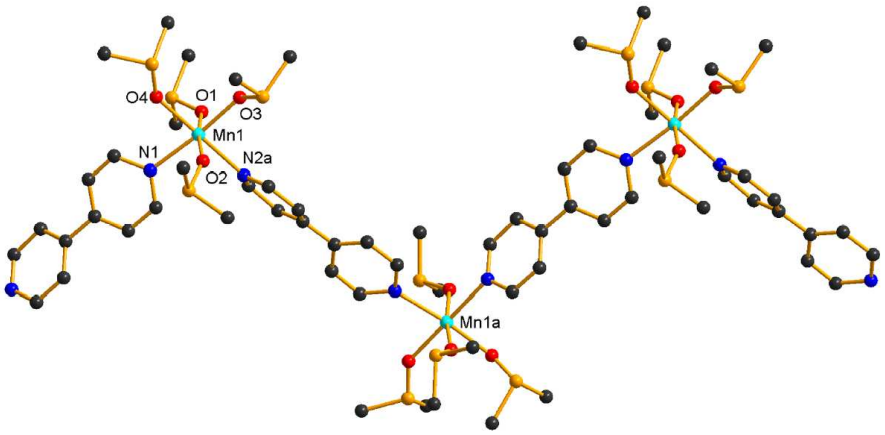

Fig. 4 Crystal structure of the zigzag polymer of $\{[Mn(4,4'\text{-bpy})(DMSO)_4]^{2+}\}_n$ in **2** with labeling scheme. Hydrogen atoms are omitted for clarity.

RSC Advances Accepted Manuscript

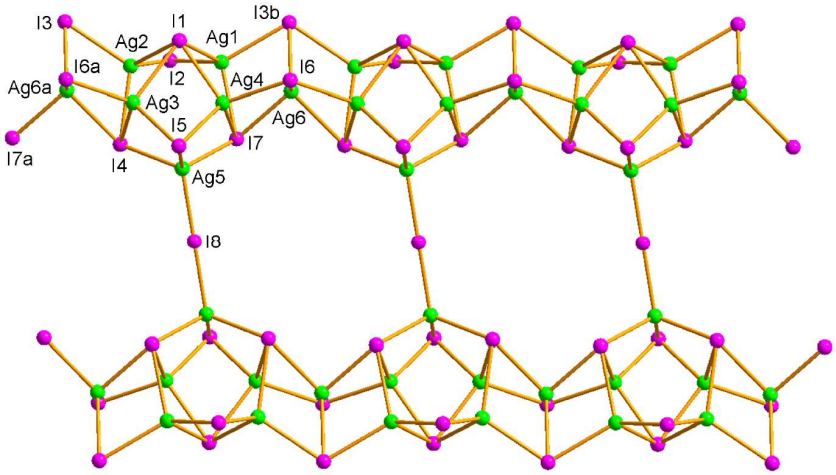

Fig. 5 Crystal structure of the $[Ag_{11}I_{15}^{4-}]_n$ chain in **2** with the labeling scheme.

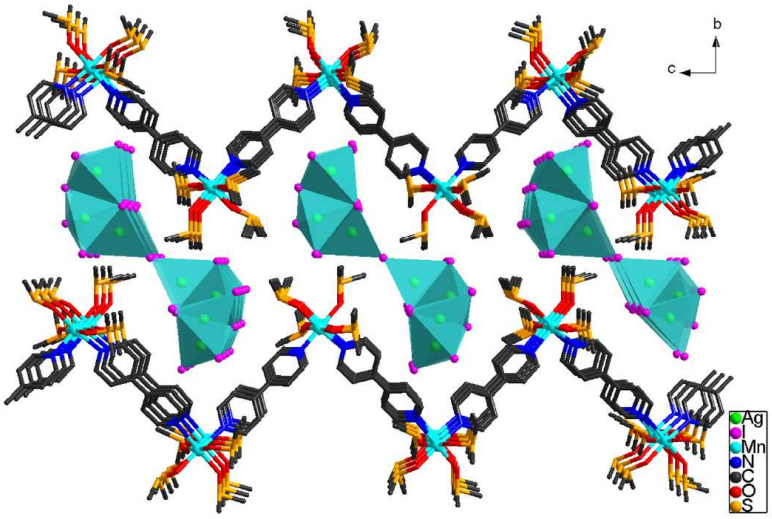

Fig. 6 View of **2** along the *a* axis. The AgI_4 units are shown as blue tetrahedra. Hydrogen atoms are omitted for clarity.

Compound **3** crystallizes in the monoclinic space group $P2_1/c$ (Table 1). It consists of a mononuclear $[Mn(4,4'\text{-bpy})_2(DMSO)_2(H_2O)_2]^{2+}$ cation, and $[Ag_{10}I_{12}^{2-}]_n$ polymeric anion, as well as two DMSO and H_2O molecules. The Mn^{2+} ion is coordinated by two 4,4′-bpy, two DMSO, and two H_2O molecules, forming an octahedral $[Mn(4,4'\text{-bpy})_2(DMSO)_2(H_2O)_2]^{2+}$ cation (Fig. 7). Unlike the 4,4′-bpy in **1** and **2**, which coordinates to Mn^{2+} ion as a bidentate bridging ligand, the 4,4′-bpy in **3** binds the Mn^{2+} ion with a monodentate coordination mode. As a result, The Mn^{2+} ion forms a mononuclear complex cation. The Mn–N and Mn–O bond lengths are consistent with corresponding bond lengths observed in compounds **1** and **2** (Tables S1−S3). Compound **3** contains five crystallographically independent Ag^+ ions, and six iodine anions (Fig. 8a). Five AgI_4 units are connected end to end by sharing common edges to form a circular Ag_5I_{12} asymmetrical unit containing a pentagram shaped ring, in which I1 shares the five Ag^+ ions. The Ag_5I_{12} units are interjoined by sharing I2, I3, I4, I5, and I6 atoms, to form the 1-D $[Ag_{10}I_{12}^{2-}]_n$ polymeric anion (Fig. 8b). All I1 anions in the $[Ag_{10}I_{12}^{2-}]_n$ chain are in the same line, and the pentagrams stack along the line. In the $[Ag_{10}I_{12}^{2-}]_n$ chain, the iodine anions adopt μ_3-I (I2–I6) or μ_5-I (I1) bridging coordination modes. The $[Ag_{10}I_{12}^{2-}]_n$ chain is isostructural with the iodoargentate anion observed in $\{[Ni(2,2'\text{-bpy})(THF)_2(H_2O)_2](Ag_{10}I_{12})\cdot 2DMF\}_n$, which contains a solvated $[Ni(2,2'\text{-bpy})]^{2+}$ unit.[6]

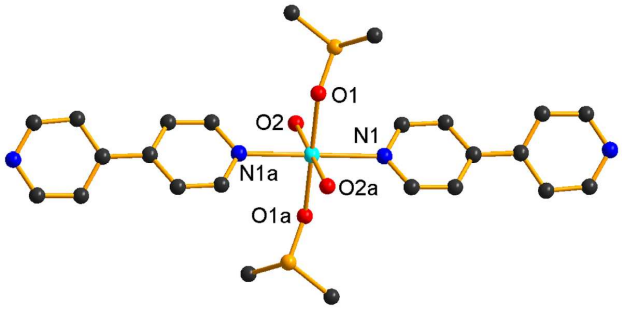

Fig. 7 Crystal structure of the $[Mn(4,4'\text{-bpy})_2(DMSO)_2(H_2O)_2]^{2+}$ cation in **3** with labeling scheme. Hydrogen atoms are omitted for clarity.

RSC Advances Accepted Manuscript

This journal is © The Royal Society of Chemistry [year]

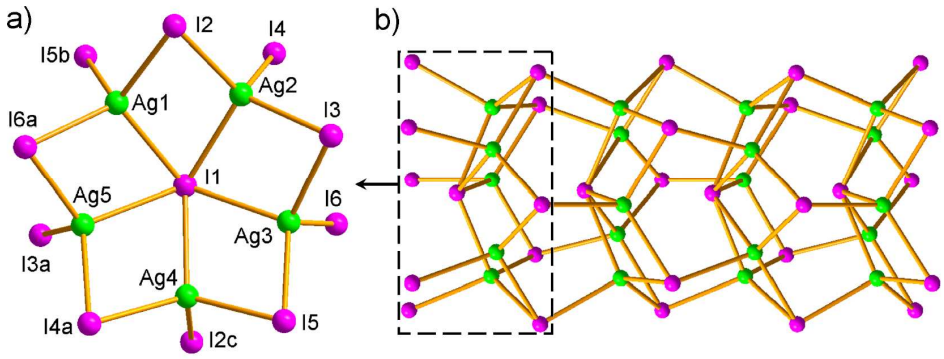

Fig. 8 (a) Crystal structure of Ag_5I_{12} asymmetrical unit with the labeling scheme in **3**. (b) Crystal structure of the $[Ag_{10}I_{12}^{2-}]_n$ chain in **3**.

In **3**, $[Mn(4,4'\text{-bpy})_2(DMSO)_2(H_2O)_2]^{2+}$, DMSO and H_2O are connected into a cationic layer perpendicular to the *a* axis via O–H···O [O···O: 2.699(9)–2.964(9) Å] and O–H···N [O···N: 2.811(11) Å] (Table S5†) intermolecular interactions (Fig. S11†). All the $[Mn(4,4'\text{-bpy})_2(DMSO)_2(H_2O)_2]^{2+}$ cations in the same layer run parallel to the *c* axis (Fig. 9). The $[Ag_{10}I_{12}^{2-}]_n$ anionic chains run along the *b* axis, and are located between the $[Mn(4,4'\text{-bpy})_2(DMSO)_2(H_2O)_2]^{2+}$/DMSO/$H_2O$ cationic layer (Fig. 9).

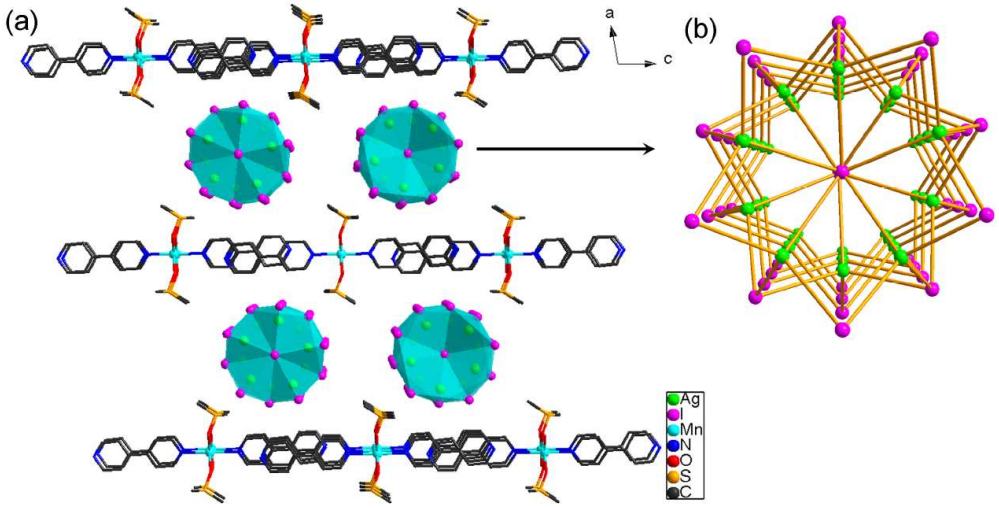

Fig. 9 (a) View of **3** along the *b* axis. The AgI_4 units are shown as blue tetrahedra. Hydrogen atoms are omitted for clarity. (b) The $[Ag_{10}I_{12}^{2-}]_n$ chain viewed along the *b* axis.

Compound **4** crystallizes in the triclinic space group *P*-1 (Table 1). It consist of a 1-D $\{[Mn_2(4,4'\text{-bpy})_2(DMSO)_2(DMF)_5(H_2O)]^{4+}\}_n$ polymeric cation, a 1-D $[Ag_{10}I_{14}^{4-}]_n$ polymeric anion, and two DMF lattice molecules. There are two crystallographically independent Mn^{2+} ions, ten Ag^+ ions, and fourteen iodine anions in **4**. $Mn(1)^{2+}$ is coordinated by two DMF and two DMSO molecules, forming a $[Mn(DMF)_2(DMSO)_2]^{2+}$ unit, while $Mn(2)^{2+}$ is coordinated by three DMF and one H_2O molecules, forming a $[Mn(DMF)_3(H_2O)]^{2+}$ unit. Acting as a bidentate bridging ligand, the 4,4′-bpy molecule interjoins $[Mn(DMF)_2(DMSO)_2]^{2+}$ and $[Mn(DMF)_3(H_2O)]^{2+}$ units to form a zigzag coordination polymer $\{[Mn_2(4,4'\text{-bpy})_2(DMSO)_2(DMF)_5(H_2O)]^{4+}\}_n$, in which $Mn(1)^{2+}$ and $Mn(2)^{2+}$ appear alternately (Fig. 10). Both $Mn(1)^{2+}$ and $Mn(2)^{2+}$ are in octahedral geometry with axial angle in the range of 170.8(10)–179.0(10)° and 173.5(12)–176.2(17)°, respectively (Table S4†). Ten AgI_4 units are connected via sharing common edges to form an $Ag_{10}I_{17}$ asymmetrical unit. The asymmetrical units are interjoined by sharing I3, I4, and I12 atoms, to form the novel 1-D $[Ag_{10}I_{14}^{4-}]_n$ polymeric anion (Fig. 11). In the $[Ag_{10}I_{14}^{4-}]_n$ chain, bridging coordination modes of μ-I (I2, I4, I5, I7, I10, I11, I14), μ_3-I (I6, I8) and μ_4-I (I1, I3, I9, I12, I13) are observed. The Ag···Ag separates in the $[Ag_{10}I_{14}^{4-}]_n$ chain are in the range of 2.834(6)–3.195(6) Å, indicating Ag···Ag interactions.

RSC Advances Accepted Manuscript

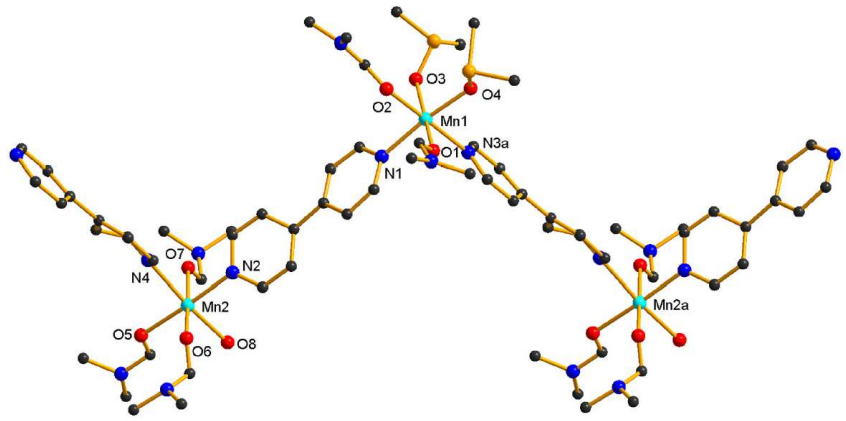

Fig. 10 Crystal structure of the zigzag polymer $\{[Mn_2(4,4'\text{-bpy})_2(DMSO)_2(DMF)_5(H_2O)]^{4+}\}_n$ in **4** with labeling scheme. Hydrogen atoms are omitted for clarity.

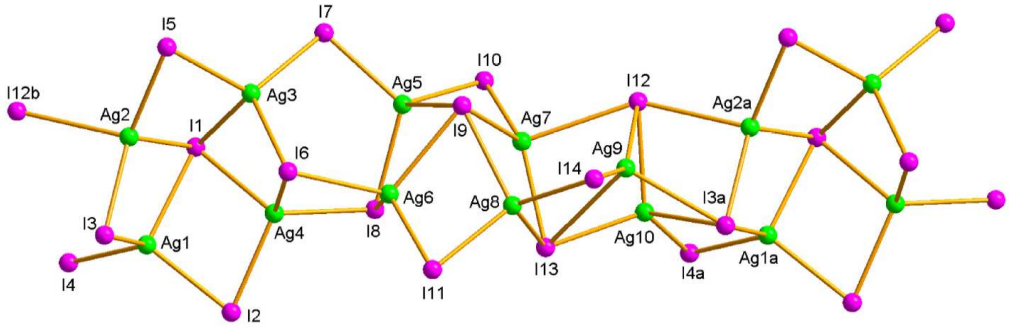

Fig. 11 Crystal structure of the $[Ag_{10}I_{14}^{4-}]_n$ chain in **4**.

The zigzag $\{[Mn_2(4,4'\text{-bpy})_2(DMSO)_2(DMF)_5(H_2O)]^{4+}\}_n$ chains run parallel to the *b* axis (Fig. 12a), and stack a cationic layer perpendicular to the *a* axis. The free DMF molecules are located between the chains. Although the Mn^{2+} ions form similar zigzag coordination polymers in **2** and **4**, the two compounds show different crystal packing. In **2**, the $[Ag_{11}I_{15}^{4-}]_n$ and $\{[Mn(4,4'\text{-bpy})(DMSO)_4]^{2+}\}_n$ chains are crossed. The $[Ag_{11}I_{15}^{4-}]_n$ anionic chains are enclosed in the channels between the zigzag $\{[Mn(4,4'\text{-bpy})(DMSO)_4]^{2+}\}_n$ cationic chains, forming a penetrating crystal packing (Fig. 8). Differently, the $[Ag_{10}I_{14}^{4-}]_n$ anionic chains in **4** are sandwiched between the cationic layers (Fig. 12a) because that the channels between the zigzag $\{[Mn_2(4,4'\text{-bpy})_2(DMSO)_2(DMF)_5(H_2O)]^{4+}\}_n$ chains are occupied by free DMF molecules, forming a sandwiched structure (Fig. 12b).

RSC Advances Accepted Manuscript

This journal is © The Royal Society of Chemistry [year]

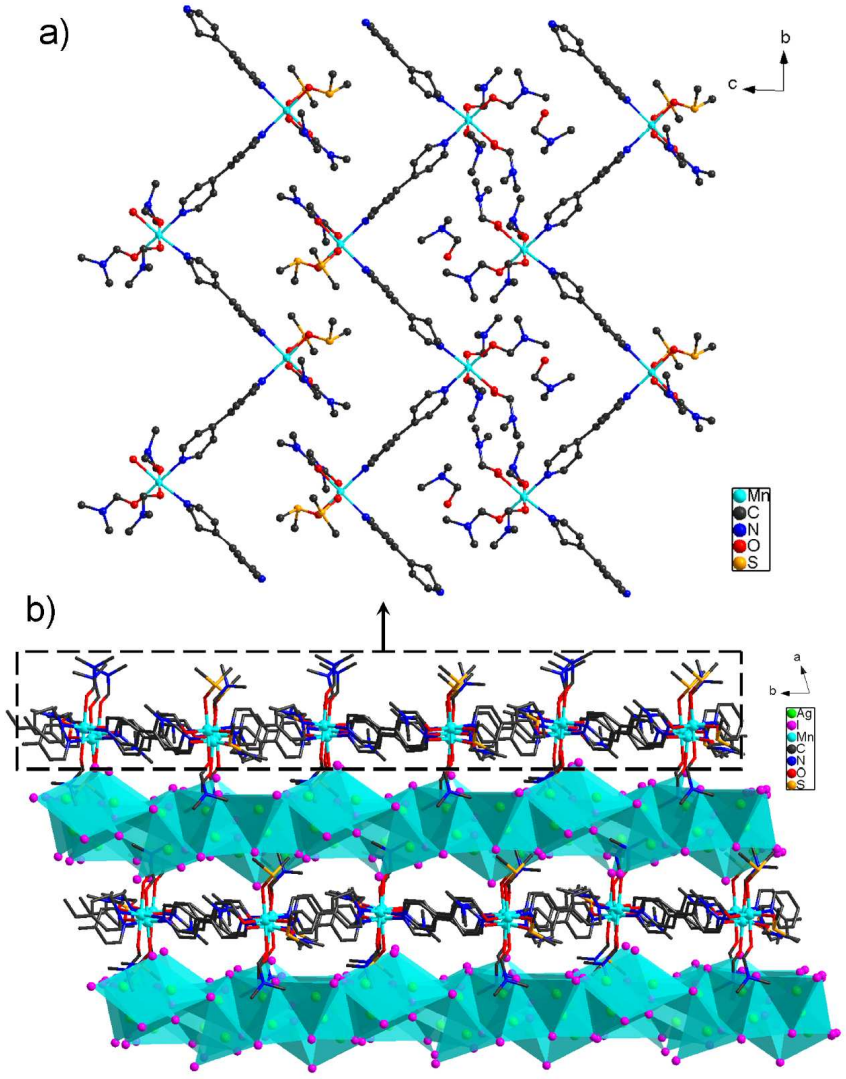

Fig.e 12 (a) Layered stacking of zigzag $\{[Mn_2(4,4'\text{-bpy})_2(DMSO)_2(DMF)_5(H_2O)]^{4+}\}_n$ chains and the free DMF molecules between the chains in **4**. (b) View of **4** along the *c* axis. The AgI_4 units are shown as blue tetrahedra. Hydrogen atoms are omitted for clarity.

A series of binary iodoargentate aggregates have been prepared by using organic cations, TM-complex cations, and Ln-complex cations as counter ions. The structures of these binary iodoargentates range from polyneclear discreted clusters $[Ag_2I_5]^{3-}$,[7a–b] $[Ag_2I_6]^{4-}$,[3a] $[Ag_3I_6]^{3-}$,[7a] $[Ag_4I_8]^{4-}$,[3b,3c,7a] 1-D chains $[Ag_2I_3^-]_n$,[3c,3d] $[Ag_2I_4^{2-}]_n$,[3e,3f,4] $[Ag_4I_6^{2-}]_n$,[3g] $[Ag_5I_7^{2-}]_n$,[3g–i, 6] $[Ag_6I_9^{3-}]_n$,[7a–b] $[Ag_{10}I_{12}^{2-}]_n$[6] and $[Ag_{12}I_{16}^{4-}]_n$,[3h], 2-D layers $[Ag_5I_6^-]_n$,[3j] $[Ag_5I_8^{3-}]_n$,[7b] to 3-D framework $[Ag_2I_4^{2-}]_n$[5], depending on the counter ions or crystallization conditions in the syntheses. Now 1-D polymeric iodoargentates $[Ag_5I_7^{2-}]_n$, $[Ag_{11}I_{15}^{4-}]_n$, $[Ag_{10}I_{12}^{2-}]_n$, and $[Ag_{10}I_{14}^{4-}]_n$ were prepared using large Mn(II) complex cations. $[Ag_{11}I_{15}^{4-}]_n$ and $[Ag_{10}I_{14}^{4-}]_n$ represent new members of the binary iodoargentate aggregates. Compound **1**, **2** and **4** are the first examples of TM-iodoargentates containing both polymeric iodoargentate anoins and polymeric cations. The polymeric anoins and cations in **1** and **2** are penetrated in the crystal packing, which have never been observed in iodoargentates. It is noteworthy that the $[Ag_5I_7^{2-}]_n$ anions can be isolated using several discrete counter ions. Now, the 1-D $[Ag_5I_7^{2-}]_n$ were obtained with polymeric $\{[Mn(4,4'\text{-bpy})(DMF)_3(H_2O)]^{2+}\}_n$ cation as template in compound **1**.

Optical absorption and photoluminescent properties

Solid-state optical absorption spectra of compounds **1**–**4** were recorded from powder samples at room temperature. The absorption data calculated the reflectance spectra using the Kubelka–Munk function[9] demonstrate that compounds **1**–**4** show well-defined abrupt absorption edges from which the band gaps can be estimated as 3.12, 3.07, 3.21, and 3.02 eV for **1**–**4**, respectively (Fig. 13). The band gaps are bigger than those of Ni- and Cu-containing iodoargentates.[7b]

RSC Advances Accepted Manuscript

The luminescent properties of **1**–**4** were measured on crystalline samples at room temperature (Fig. 14). When excited at 270 nm, **1** and **3** exhibit a strong photoluminescent emission band at 458, and 449 nm, respectively. Compounds **2** and **4** give an emission band at 487 and 475 nm respectively, on excited at 280 nm. According to the results for similar hybrid iodoargentates,[3g, 6, 13] the emission bands can be assigned to the mixture of metal-to-metal transfer (Ag 5s or 5p-to-Ag 4d) and iodide-to-metal charge transfer (I 5p-to-Ag 4d) and affected by the metal-metal interactions. The emission bands shift to the red from **3** to **1**, and to **2** and **4**. The red shift was attributed to stronger silver-silver interactions in the $[Ag_{11}I_{15}^{4-}]_n$ and $[Ag_{10}I_{14}^{4-}]_n$ chains, manifested by the shorter Ag···Ag separates. This situation is similar to the observed red shift from chair $(Ph_3P)_4Ag_4I_4$ to the cube $(Ph_3P)_4Ag_4I_4$ with more silver-silver interactions.[13a]

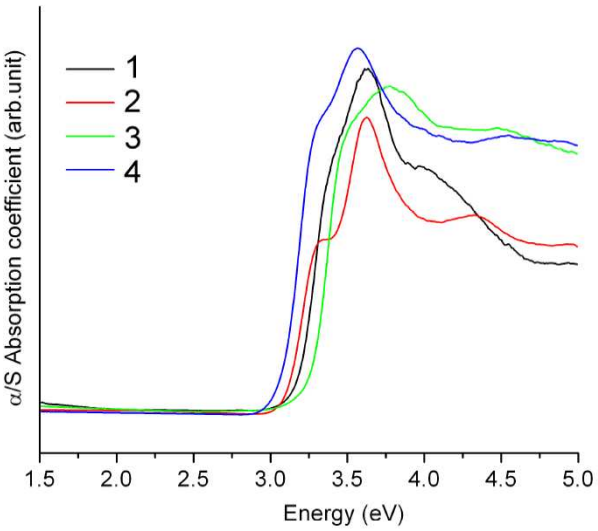

Fig. 13 Optical absorption spectra of compounds **1**−**4**.

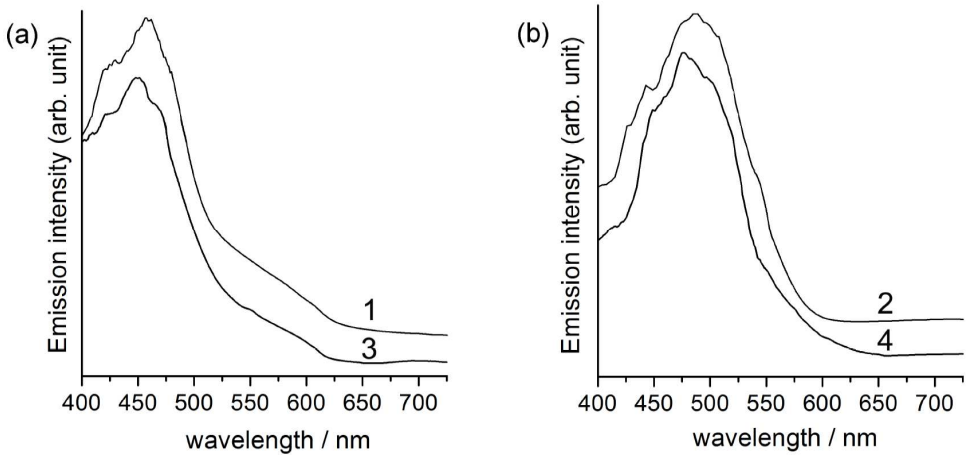

Fig. 14 Solid state emission spectra of compounds **1**–**4** at room temperature. The photoluminescent spectra were excited by 270 nm (**1**, **3**), and 280 nm (**2**, **4**) lights

Thermal properties

Thermal gravimetric analyses of compounds **1**–**4** were investigated under a nitrogen atmosphere in the temperature range of 25–500°C, and the TAG curves are shown in Fig. S12†. Compound **1** decomposes in multi-steps. It loses free 4,4′-bpy molecule (weight loss: theoretical 7.7%, observed 7.5%) between 120 and 215 °C. In the subsequent steps, it loses three DMF and one H_2O ligands in 225–290 °C, and 4,4′-bpy ligand in 300–380 °C. Compound **2** decomposes in two steps. The observed total mass losses of 24.3% corresponds to the losses of eight DMSO (15.1%) and two 4,4′-bpy (7.6%) ligands. Compound **3** starts losing free H_2O molecule at about 100 °C and loses two H_2O and two DMSO molecules before 220 °C. In the subsequent steps, it gradually loses two H_2O and two DMSO ligands, followed by loss of two 4,4′-bpy ligands. The observed total mass losses of 20.7% matches with the theoretical value for complete removal of all the ligands and solvent molecules. Like compound **3**, **4** also exhibits a multi-step decomposition process. The total mass losses of 26.7% are in accordance with the removal of two free DMF (3.7%) molecules in the first step, DMF, DMSO and H_2O ligands (13.6%) in the second and third step, and two 4,4′-bpy ligands (7.9%) in the fourth step.

Conclusions

In summary, solvent effects on the system AgI/KI/Mn^{2+}/4,4′-bpy were observed. Polymeric iodoargentates **1**, **2**, **3** and **4** were obtained by the reaction of AgI and KI in different mixed polar solvents and crystallization with large Mn(II) complex cations, indicating the influence of solvated $[Mn(4,4'\text{-bpy})]^{2+}$ cation on the self-assembly of iodoargentates. The $[Mn(4,4'\text{-bpy})]^{2+}$ cations solvatetd with different solvent molecules led to 1-D polymeric iodoargentate anions $[Ag_5I_7^{2-}]_n$, $[Ag_{11}I_{15}^{4-}]_n$, $[Ag_{10}I_{12}^{2-}]_n$, and $[Ag_{10}I_{14}^{4-}]_n$, among which $[Ag_{11}I_{15}^{4-}]_n$ and $[Ag_{10}I_{14}^{4-}]_n$ represent new members of binary iodoargentate aggregates. These results illustrate the potential of using TM complex cations modified by small solvent ligands to tune the structure and compositions of iodometallate anions.

RSC Advances Accepted Manuscript

This journal is © The Royal Society of Chemistry [year]

Acknowledgements

This work was supported by the National Natural Science Foundation of P. R. China (Nos. 21171123), and the Priority Academic Program Development (PAPD) of Jiangsu Higher Education Institutions

Notes and references

[a]*College of Chemistry, Chemical Engineering and Materials Science, Dushu Lake Campus, Soochow University, Suzhou 215123, People's Republic of China. Fax/Tel: + 86-512-65880089; E-mail: jiadingxian@suda.edu.cn*

† Electronic Supplementary Information (ESI) available: selected bond lengths and angles for **1**–**4**, IR spectra, PXRD patterns, structural figures, and TG curves. CCDC reference numbers 995786–995789 for **1**–**4**. Crystallographic data in CIF. See DOI: 10.1039/b000000x/

1 (*a*) D. B. Mitzi, C. A. Feild, W. T. A. Harrison and A. M. Guloy, *Nature,* 1994, **369**, 467–469; (*b*) D. B. Mitzi, S. Wang, C. A. Feild, C. A. Chess and A. M. Guloy, *Science,* 1995, **267**, 1473–1476; (*c*) C. R. Kagan, D. B. Mitzi and C. D. Dimitrakopoulos, *Science,* 1999, **286**, 945–947; (*d*) G. C. Papavassiliou, *Prog. Solid State Chem.,* 1997, **25**, 125–270; (*e*) C. H. Arnby, S. Jagner and I. Dance, *CrystEngComm.,* 2004, **6**, 257–275; (*f*) J. L. Knutson, J. D. Martin and D. B. Mitzi, *Inorg. Chem.,* 2005, **44**, 4699–4705; (*g*) A. Kojima, K. Teshima, Y. Shirai and T. Miyasaka, *J. Am. Chem. Soc.,* 2009, **131**, 6050–6051.

2 (*a*) S. Wang, D. B. Mitzi, C. A. Feild and A. M. Guloy, *J. Am. Chem. Soc.,* 1995, **117**, 5297–5302; (*b*) D. B. Mitzi, *Chem. Mater.,* 1996, **8**, 791–800; (*c*) N. Mercier, S. Poiroux, A. Riou and P. Batail, *Inorg. Chem.,* 2004, **43**, 8361–8366; (*d*) N. Mercier, A. L. Barres, M. Giffard, I. Rau, F. Kajzar and B. Sahraoui, *Angew. Chem. Int. Ed.,* 2006, **45**, 2100–2103; (*e*) S. Sourisseau, N. Louvain, W. Bi, N. Mercier, D. Rondeau, F. Boucher, J.-Y. Buzaré and C. Legein, *Chem. Mater.,* 2007, **19**, 600–607; (*f*) C. C. Stoumpos, C. D. Malliakas and M. G. Kanatzidis, *Inorg. Chem.,* 2013, **52**, 9019–9038; (*g*) T. Baikie, Y. Fang, J. M. Kadro, M. Schreyer, F. Wei, S. G. Mhaisalkar, M. Graetzel and T. J. White, *J. Mater. Chem. A,* 2013, **1**, 5628–5641.

3 (*a*) J. F. Bringley, M. Rajeswaran, L. P. Olson and N. M. Liebert, *J. Solid State Chem.,* 2005, **178**, 3074–3089; (*b*) S. Olson, G. Helgesson and S. Jagner, *Inorg. Chim. Acta.,* 1994, **217**, 15–20; (*c*) G. C. Papavassiliou, G. A. Mousdis, A. Terzis and C. P. Raptopoulou, *Z. Naturforsch.,* 1999, **54b**, 109–112; (*d*) H. Paulsson, M. Berggrund, A. Fischer and L. Kloo, *Eur. J. Inorg. Chem.,* 2003, 2352–2355; (*e*) H. H. Li, Z. R. Chen, C. C. Huang, Y. G. Ren and Q. H. Chen, *Chin. J. Struct. Chem.,* 2004, **23**, 288–291; (*f*) H. H. Li, Z. R. Chen, C. C. Huang, Y. G. Ren and G. C. Xiao, *Chin. J. Struct. Chem.,* 2004, **23**, 1009–1012; (*g*) H. H. Li, Z. R. Chen, J. Q. Li, C. C. Huang, Y. F. Zhang and G. X. Jia, *Cryst. Growth Des.,* 2006, **6**, 1813–1820; (*h*) H.-H. Li, Z.-R. Chen, J.-Q. Li, C.-C. Huang, Y.-F. Zhang and G.-X. Jia, *Eur. J. Inorg. Chem.,* 2006, 2447–2453; (*i*) N. Kuhn, Q. Abu-Salem, C. Maichle-Mößmer and H. Schubert, *Z. Kristallogr. NCS.,* 2008, **223**, 341–342; (*j*) E. Cariati, R. Macchi, D. Roberto, R. Ugo, S. Galli, N. Masciocchi and A. Sironi, *Chem. Mater.,* 2007, **19**, 3704–3711.

4 L. G. Li, H. H. Li, Z. R. Chen, C. C. Huang, B. Zhao and J. Q. Li, *Chin. J. Struct. Chem.,* 2006, **25**, 149–152.

5 Y. S. Jiang, H. G. Yao, S. H. Ji, M. Ji and Y. L. An, *Inorg. Chem.,* 2008, **47**, 3922–3924.

6 H. H. Li, Z. R. Chen, L. G. Sun, Z. X. Lian, X. B. Chen, J. B. Li and J. Q. Li, *Cryst. Growth Des.,* 2010, **10**, 1068–1073.

7 (*a*) S. Mishra, E. Jeanneau, S. Daniele and G. Ledoux, *Dalton Trans.,* 2008, 6296–6304; (*b*) S. Mishra, E. Jeanneau, G. Ledoux and S. Daniele, *Dalton Trans.,* 2009, 4954–4961.

8 (*a*) H. Krautscheid and F. Vielsack, *Angew. Chem. Int. Ed.,* 1995, **34**, 2035–2037; (*b*) H. Krautscheid and F. Vielsack, *Z. Anorg. Allg. Chem.,* 1997, **623**, 259–263; (*c*) H. Krautscheid and F. Vielsack, *J. Chem. Soc., Dalton Trans.,* 1999, 2731–2735; (*d*) N. Louvain, W. Bi, N. Mercier, J.-Y. Buzaré, C. Legein and G. Corbel, *Dalton Trans.,* 2007, 965–970.

9 W. W. Wendlandt and H. G. Hecht, *Reflectance Spectroscopy*; Interscience Publishers: New York, 1966.

10 (*a*) G. M. Sheldrick, *SHELXS-97, Program for Crystal Structure Determination*; University of Göttingen: Germany, 1997; (*b*) G. M. Sheldrick, *SHELXL-97, Program for the Refinement of Crystal Structures*; University of Göttingen: Germany, 1997.

11 (*a*) X. Li, X. Zhao, Y. Bing, M. Zha, H. Xie and Z. Guo, *J. Solid State Chem.,* 2013, **197**, 81–91; (*b*) Y. S. Ma, X. Y. Tang, F. F. Xue, B. Chen, Y. L. Dai, R. X. Yuan and S. Roy, *Eur. J. Inorg. Chem.,* 2012, 1243–1249; (*c*) D. Li, S. Parkin, G. Wang, G. T. Yee, A. V. Prosvirin and S. M. Holmes, *Inorg. Chem.,* 2005, **44**, 4903–4905.

12 A. Bondi, *J. Phys. Chem. B.,* 1964, **68**, 441–451.

13 (*a*) M. Henary and J. I. Zink, *Inorg. Chem.,* 1991, **30**, 3111–3112; (*b*) V. J. Catalano, H. M. Kar and J. Garnas, *Angew. Chem. Int. Ed.,* 1999, **38**, 1979–1982.

RSC Advances Accepted Manuscript

Graphical Abstarct.

Table of Contents Synopsis

Novel polymeric iodoargentates $[Mn(4,4'\text{-bpy})(DMF)_3(H_2O)]$ $Ag_5I_7 \cdot 4,4'\text{-bpy}$ (**1**), $[Mn(4,4'\text{-bpy})(DMSO)_4]_2Ag_{11}I_{15}$ (**2**), $[Mn(4,4'\text{-bpy})_2(DMSO)_2(H_2O)_2]Ag_{10}I_{12} \cdot 2DMSO \cdot 2H_2O$ (**3**), and $[Mn_2(4,4'\text{-bpy})_2(DMF)_5(DMSO)_2(H_2O)]Ag_{10}I_{14} \cdot 2DMF$ (**4**) were prepared templated by $[Mn(4,4'\text{-bpy})]^{2+}$ solvated with different solvent molecules.

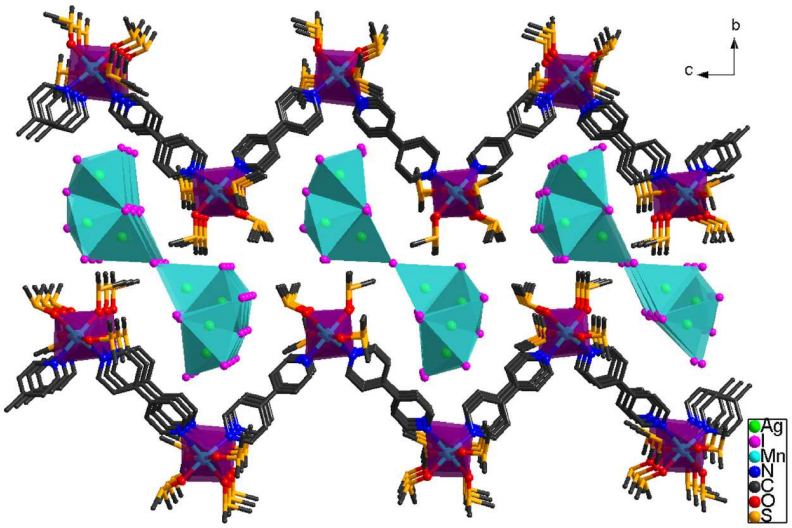

RSC Advances Accepted Manuscript